Molecular Crystals and Liquid Crystals
Publication details, including instructions for authors and subscription information:
http://www.tandfonline.com/loi/gmcl20

Temperature-Dependent, High-Resolution Magic-Angle-Spinning (HRMAS) NMR Studies of Poly(N-isopropylacrylamide-co-acrylic Acid)

Christopher M. Burba [a] & Charles V. Rice [b]

[a] Department of Natural Sciences, Northeastern State University, 600 N. Grand Ave, Tahlequah, OK, 74464, USA

[b] Department of Chemistry and Biochemistry, University of Oklahoma, Stephenson Life Sciences Research Center, 101 Stephenson Parkway, Norman, OK, 73019, USA

Available online: 14 Feb 2012

To cite this article: Christopher M. Burba & Charles V. Rice (2012): Temperature-Dependent, High-Resolution Magic-Angle-Spinning (HRMAS) NMR Studies of Poly(N-isopropylacrylamide-co-acrylic Acid), Molecular Crystals and Liquid Crystals, 555:1, 280-294

To link to this article: http://dx.doi.org/10.1080/15421406.2012.635558

Mol. Cryst. Liq. Cryst., Vol. 555: pp. 280–294, 2012

ISSN: 1542-1406 print/1563-5287 online
DOI: 10.1080/15421406.2012.635558

Taylor & Francis
Taylor & Francis Group

Temperature-Dependent, High-Resolution Magic-Angle-Spinning (HRMAS) NMR Studies of Poly(*N*-isopropylacrylamide-*co*-acrylic Acid)

CHRISTOPHER M. BURBA[1,*] AND CHARLES V. RICE[2]

[1]Department of Natural Sciences, Northeastern State University, 600 N. Grand Ave, Tahlequah, OK 74464 USA
[2]Department of Chemistry and Biochemistry, University of Oklahoma, Stephenson Life Sciences Research Center, 101 Stephenson Parkway, Norman, OK, 73019 USA

*High-resolution magic-angle-spinning NMR spectroscopy is used to investigate the phase transition of poly(*N*-isopropylacrylamide-co-acrylic acid) hydrogels crosslinked with N,N'-methylene bisacrylamide, hereafter poly(NIPAAm-co-AAc). Van't Hoff ΔH and ΔS for polymer dehydration are derived from temperature-dependent NMR spectra, and the thermodynamic data strongly support a four-stage dehydration mechanism for pure poly(NIPAAm). Acrylic acid stabilizes the hydration sphere around the polymer chains. Reduced amounts of water released during the phase transition translates into smaller values for ΔH and ΔS. Enhanced rehydration kinetics for poly(NIPAAm-co-AAc) is attributed to water remaining in the samples at elevated temperatures, which may produce facile diffusion pathways and enable faster rehydration kinetics than poly(NIPAAm).*

Keywords acrylic acid; HRMAS NMR spectroscopy; hydrogels; kinetics; poly (*N*-isopropylacrylamide); thermodynamics

Introduction

Tremendous research efforts are devoted to the development of polymers that respond to external stimuli (e.g., temperature and pH) for physiological applications [1–7]. Alkyl acrylamide-based polymers, especially poly(*N*-isopropylacrylamide or poly(NIPAAm), are among the most heavily investigated of these families for drug delivery or tissue engineering applications. The good biocompatibility of poly(NIPAAm) coupled with a sharp phase separation at its lower critical solution temperature (LCST, 32°C) has contributed much to the success of this polymer [8]. Lower critical phase separation is typically viewed as a delicate balance between the hydrophilic and hydrophobic moieties of the polymer chain. At room temperature, the polymer chains of poly(NIPAAm) are surrounded by a hydration shell that stabilizes the system through extensive hydrogen-bonding interactions between water molecules and the amide groups of the NIPAAm substituents. However, heating the polymer destabilizes the hydration shell, leading to rapid dehydration and phase separation

*Address correspondence to Dr. Christopher M. Burba, Department of Natural Sciences, Northeastern State University, 600 N. Grand Ave, Tahlequah, OK 74464 USA. Tel. 918-444-3835; Fax. 918-458-2325. E-mail: burba@nsuok.edu

at its LCST. In crosslinked poly(NIPAAm), the phase transition is marked by a significant volume change as the translucent, swollen hydrogel becomes an opaque, insoluble solid.

One avenue of research in developing this field of biomaterials is to copolymerize NIPAAm with acrylic acid (AAc). Here, the goal is to use the acrylic acid sites to attach physiologically relevant molecules to the polymer backbone, allowing poly(NIPAAm-*co*-AAc) hydrogels to function as a scaffold for tissue regeneration [9–11]. However, copolymers of NIPAAm and acrylic acid exhibit different phase behavior from poly(NIPAAm), even at very low doping levels. Acrylic acid increases the overall hydrophilicity of the polymer chains, thus raising the LCST of the hydrogel and decreasing the extent of the temperature-induced volume change [12]. As these effects may impede future physiological applications of these materials, it is very important to have a good molecular-level understanding of how acrylic acid influences the phase transition behavior of poly(NIPAAm) hydrogels to better address these issues.

In this work, nuclear magnetic resonance (NMR) spectroscopy is used to quantitatively measure the van't Hoff enthalpy and entropy of the phase transition process for poly(NIPAAm-*co*-AAc) in D_2O. In the fully hydrated state ($T <$ LCST), the molecular units composing the polymer chains are relatively flexible and any chemical shift anisotropy (CSA) or dipole-dipole coupling effects that exist in the sample may be removed with high-resolution magic-angle-spinning (HRMAS) NMR methods [13–18]. However, the CSA and dipole-dipole coupling effects become very strong in the collapsed state (i.e., $T >$ LCST) and solution NMR probes do not deliver high enough radio frequency (rf) power to study those portions of the sample. Consequently, no NMR signal is detected for dehydrated segments of the polymer. The relative amounts of flexible, hydrated NIPAAm segments within the sample are directly measured by following the intensity of methyl protons from the NIPAAm substituents with HRMAS ^{1}H NMR spectroscopy. Thus, a quantitative assessment of how acrylic acid influences the phase transition during heating and cooling cycles is available from the perspective of the NIPAAm constituents. A similar strategy was used to evaluate thermodynamic properties of the phase transition process for poly(NIPAAm) in D_2O [14] and in D_2O salt solutions [13].

Experimental Methods

Materials

N-isopropylacrylamide (NIPAAm, 97%), *N*,*N*′-methylene bisacrylamide (MBAAm, 98%), *N*,*N*,*N*′,*N*′-tetramethylenediamine (TEMED, 99%), and acrylic acid (AAc, 99%) were purchased from Aldrich. Riboflavin 5′-phosphate was purchased from Spectrum, and deuterium oxide (D_2O) was obtained from Cambridge Isotopes Laboratories. All reagents were used as received, and solutions were prepared with doubly distilled H_2O.

Polymerization

Poly(NIPAAm-*co*-AAc) hydrogels were synthesized by photo-polymerization of NIPAAm, AAc, and MBAAm. Nominal acrylic acid doping levels of 0.0, 1.0, 2.5, 5.0, and 10.0 mol% were prepared. In a typical synthesis, 2.00 mL of NIPAAm solution (0.7899 M) was mixed with an appropriate quantity of acrylic acid. Afterwards, a sufficient volume of 41.3 mM MBAAm was added to prepare a gel with a crosslinking density of 300:1, defined as (moles of NIPAAm + moles of AAc):moles of MBAAm. This was followed by the addition of 100 μL of 1.0 mM Riboflavin 5′-phosphate and 10 μL of pure TEMED

as initiators. The resulting solutions were intimately mixed and neutralized until pH = 7. Photo-polymerization was performed for 30 min at 254 nm using a Spectroline® UV Crosslinker Select™ (Fisher Scientific). The resulting hydrogels were thoroughly washed by heating the gel above the LCST and then rehydrating the gel with doubly distilled H_2O. This process was repeated at least three times to remove excess reagents.

NMR Spectroscopy

Small quantities (∼50 μL) of dehydrated poly(NIPAAm-*co*-AAc) were placed in a ceramic, high-resolution magic-angle-spinning (HRMAS) rotor, and the gels were then allowed to rehydrate in the presence of D_2O for approximately 1 h. NMR spectra were collected using a Varian $^{13}C\{^1H\}$ HRMAS NanoProbe® and a Mercury VX 300 MHz NMR Spectrometer. VnmrJ 1.1D software (Varian, Inc.) was used for data collection and processing. The ^1H chemical shift values were referenced to the residual water signal (HOD) at 4.8 ppm. Temperature calibration of the NMR spectrometer was accomplished with the temperature-dependent chemical shift of ethylene glycol, and all samples were spun at a rate of ∼2000 Hz. During variable-temperature NMR measurements (both heating and cooling cycles), the samples were allowed to rest 5 minutes at each temperature prior to acquiring the spectra.

Deuterium lock was maintained throughout data acquisition to control the field frequency ratio over the sample [18–20]. Temperature-induced changes in solvent density affect the magnetic susceptibility of the sample. This can change the intensity of the local magnetic field at the sample, influencing measured chemical shift values. Furthermore, changes in probe temperature also create magnetic inhomogeneities that may result in peak broadening and/or splitting. These effects are removed by sample shimming on the deuterium signal at each temperature interval.

Results

Effect of Acrylic Acid on the Phase Transition Temperature

HRMAS NMR spectra of poly(NIPAAm-*co*-AAc) consist of four peaks in addition to the intense peak due to residual water molecules (HOD, 4.8 ppm). Peak assignments have been previously reported and are adopted here [14]. The methyl protons of the NIPAAm groups (ca. 1.05 ppm) are the strongest signal in the NMR spectrum and also participate in hydrophobic bonds that are created as the temperature is increased. Hence, normalized peak intensities of this signal are used to follow changes in the hydrogel as a function of temperature and acrylic acid content; similar results are obtained if other signals are used. Variable temperature NMR measurements for several poly(NIPAAm-*co*-AAc) hydrogels are presented in Fig. 1. The peak intensity of poly(NIPAAm) remains constant between 23 and 31°C. At these temperatures, the polymer chains are hydrated and flexible, thus a ^1H NMR signal is detected. However, the cross-linked polymer rapidly dehydrates and becomes rigid near its LCST. This is accompanied by a precipitous decrease in the intensity of the NMR peaks, after which no signal is detected. The addition of acrylic acid causes an increase in the measured LCST of poly(NIPAAm) [21, 22]. For instance, the midpoints of the normalized signals increase from 33°C for poly(NIPAAm) to 39°C for 5.0 mol% poly(NIPAAm-*co*-AAc) sample. In addition, polymer dehydration occurs over a broader range of temperatures for poly(NIPAAm-*co*-AAc) materials compared to pure poly(NIPAAm).

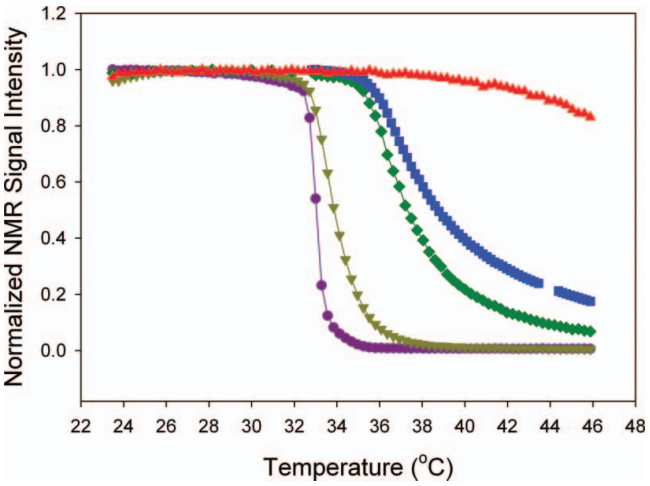

Figure 1. Temperature-dependent HRMAS ^{1}H NMR data for poly(NIPAAm-*co*-AAc) hydrogels as a function of acrylic acid content. Normalized signal intensities are reported for the methyl protons on the *N*-isopropylacrylamide substituents ($\delta = 1.05$ ppm). Samples are denoted by the acrylic acid contents (reported in mole percent) as follows: ● = 0.0, ▼ = 1.0, ◆ = 2.5, ■ = 5.0, and ▲ = 10.0.

The addition of hydrophilic acrylic acid sites along the polymer chains will undoubtedly affect inter- and intramolecular properties of the copolymers and, as a consequence, the chemical and physical properties of hydrogels. A number of poly(NIPAAm)-based binary [22–25] and ternary [12, 26, 27] polymer systems show variations in the LCSTs. In general, hydrophilic co-monomers increased LCSTs by stabilizing the hydration shell around the polymer chains. In contrast, hydrophobic co-monomers destabilized the hydration shell and lowered the LCSTs. At the doping levels investigated here, the poly(NIPAAm-*co*-AAc) samples may be viewed as relatively long chains of NIPAAm interspersed with hydrophilic acrylic acid sites. Hydrogels containing small quantities of acrylic acid (<1.0 mol%) consist of fairly long segments of repeating NIPAAm monomeric units. Consequently, the phase behavior of the 1.0 mol% copolymer is slightly perturbed compared to poly(NIPAAm). As the acrylic acid content increases, the average size of the NIPAAm segments decreases, and the acrylic acid sites exert a stronger influence on the hydration shell of the polymer chains.

Residual NMR signal intensity for dehydrated samples is a direct measure of the amount of hydrated polymer chains present in the collapsed phase. The NMR signal from the methyl protons of NIPAAm persists at elevated temperatures for high doping levels of acrylic acid (5.0 and 10.0 mol%). Indeed, the 10.0 mol% sample only slightly dehydrates over the temperature range of the NMR probe, leaving most of the NIPAAm monomeric units hydrated and relatively flexible. Figure 2 shows the fraction of hydrated NIPAAm substituents as a function of AAc-doping level at 46°C—near the high temperature limit of the HRMAS NMR probe. At a 10.0 mol% doping level, most of the NIPAAm segments are small, and strong water-acrylic acid hydrogen bonds prevent significant dehydration of the hydrogel. Consequently, approximately 84% of the polymer remains hydrated. Even in boiling water, only a small portion of the sample was visually observed to collapse. The stabilization of the hydration shell is less extensive in samples containing smaller quantities of acrylic acid. For example, approximately 17% of NIPAAm remains hydrated at elevated

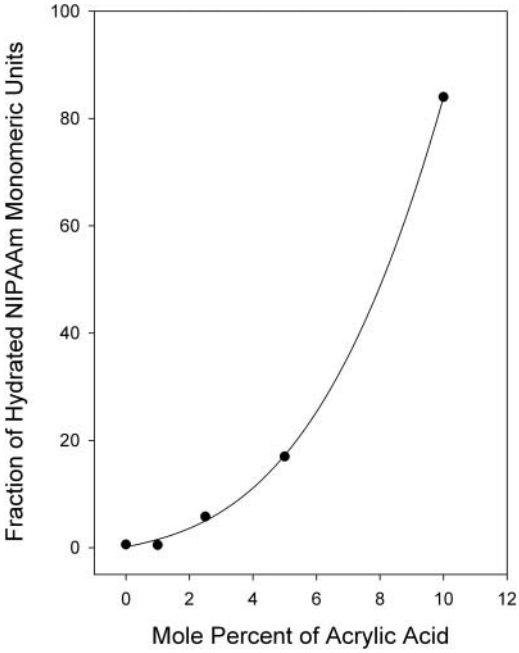

Figure 2. The fraction of hydrated NIPAAm monomeric units, as measured by HRMAS ^{1}H NMR spectroscopy at 46°C, is plotted as a function of acrylic acid content. A best fit trend line is included.

temperatures for a doping level of 5.0 mol%. The observation of significant changes in the temperature-dependent ^{1}H NMR intensity profiles confirms the notion that small quantities of acrylic acid can exert large effects on the stability of the hydration shell surrounding the polymer chains.

Thermodynamics of Dehydration

HRMAS ^{1}H NMR spectra provide additional insight into the phase transition thermodynamics of poly(NIPAAm-*co*-AAc) hydrogels. As noted in Fig. 1, the polymer chains yield measurable ^{1}H NMR signals when hydrated, but the intensity of the NMR peaks rapidly decrease over the phase transition for samples containing small amounts of acrylic acid (<5.0 mol%). Because peak signals are due solely to flexible, hydrated portions of the polymer, the normalized peak intensities may be used to directly measure the equilibrium constant, K_{eq}, for the reaction poly(NIPAAm-*co*-AAc)$_{\text{hydrated}} \rightleftharpoons$ poly(NIPAAm-*co*-AAc)$_{\text{collapsed}}$. In terms of the NMR signal, denoted S, the equilibrium constant may be defined as

$$K_{eq} = \frac{\left[\text{poly(NIPAAm-}co\text{-AAc)}_{collapsed}\right]}{\left[\text{poly(NIPAAm-}co\text{-AAc)}_{hydrated}\right]} = \frac{S_o - S}{S}. \tag{1}$$

The value of $S_o = 1$ when the NMR spectra are normalized with respect to the maximum signal intensity. Van't Hoff plots for cross-linked poly(NIPAAm-*co*-AAc) hydrogels with acrylic acid contents of 0.0, 1.0 and 2.5 mol% are depicted in Fig. 3. The 5.0 and 10.0 mol% samples are not included in the analysis because the temperature limit of the NMR probe

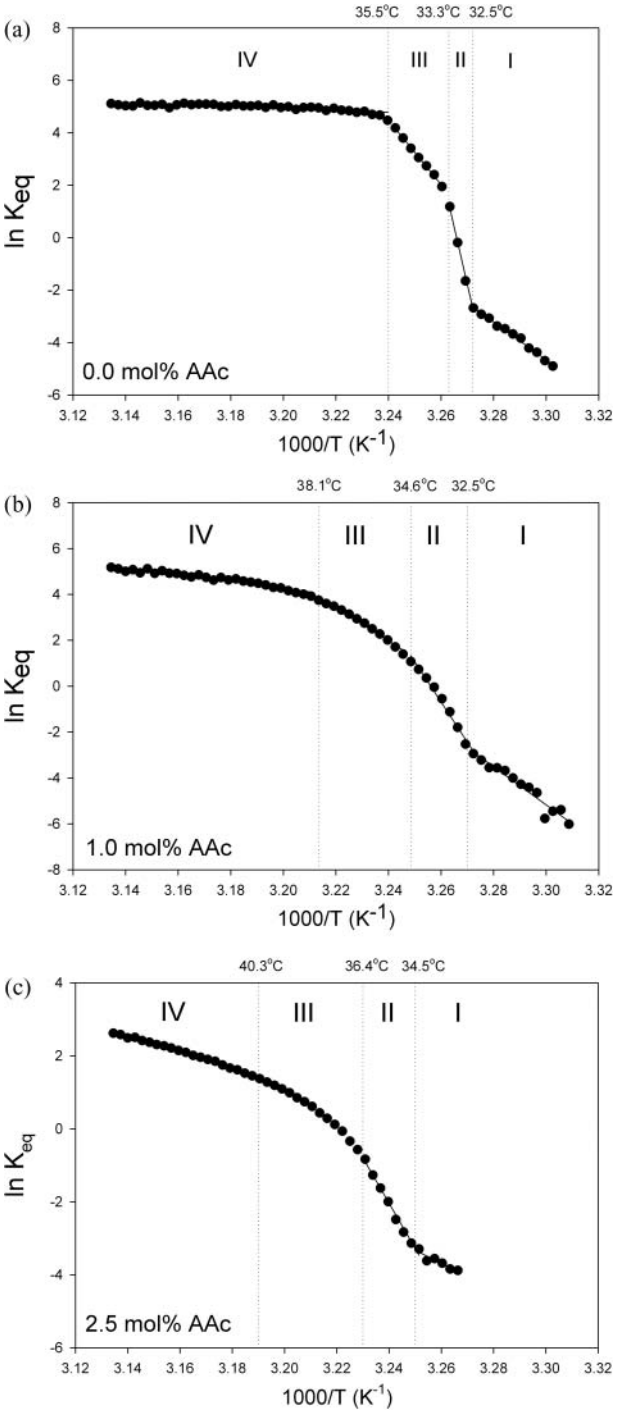

Figure 3. Van't Hoff plots of poly(NIPAAm-*co*-AAc) are provided for hydrogels containing (a) 0.0, (b) 1.0, and (c) 2.5 mol% acrylic acid.

is too low to fully dehydrate the compounds. Thus, a substantial portion of the dehydration process is unavailable.

Four distinct linear domains are indentified in the van't Hoff plots for pure poly(NIPAAm), and each region is denoted in Fig. 3 with Roman numerals. Region I corresponds to temperatures below 32.4°C, which is before the precipitous decrease in NMR signal intensity shown in Fig. 1 for this sample. Therefore, region I is assigned to pre-phase transition changes within the hydrogel. Region II ranges from 32.5 to 33.3°C. During this temperature range, poly(NIPAAm) undergoes substantial dehydration, corresponding to significant loss in the NMR signal. A third linear region observed between 33.3 and 35.5°C is assigned to post-phase transition changes in the hydrogel. Region IV for poly(NIPAAm) has essentially zero slope because the sample is almost fully dehydrated at these temperatures. Consequently, no measurable NMR signal is detected. The sample is a relatively rigid, opaque solid over this region. Van't Hoff plots for poly(NIPAAm-*co*-AAc) samples show the same qualitative trends as poly(NIPAAm), and the van't Hoff plots are also divided into four regions for comparison with the poly(NIPAAm) data. Regions II, III and IV are less well defined in the copolymerized materials compared to poly(NIPAAm). This is especially evident for region III, where the data displays significant curvature in the ln K_{eq} versus 1/T graphs. Statistically significant linear correlations ($p < 0.05$) are identified in regions I, II and IV for both 1.0 and 2.5 mol% samples.

Temperature-dependent measurements of the equilibrium constant may be used to calculate the enthalpy and entropy changes associated with the phase transition process using the van't Hoff equation:

$$\ln K_{eq} = -\frac{\Delta H}{RT} + \frac{\Delta S}{R}. \tag{2}$$

Van't Hoff enthalpy and entropy changes associated with regions I-IV for poly (NIPAAm)and regions I, II and IV for poly(NIPAAm-*co*-AAc) are calculated from best-fit linear equations to the data presented in Fig. 3 and summarized in Table 1. It is not uncommon for the van't Hoff enthalpy to be substantially different from the enthalpy measured through calorimetry, particularly for macromolecules [28]. In most cases, the discrepancy lies with the cooperativity of many monomeric units contributing to the van't Hoff enthalpy, whereas the calorimetric enthalpy is taken to be a measure of the enthalpy per monomeric unit. The concept of a cooperative unit may begin to break down somewhat in the context of a cross-linked hydrogel, further obfuscating the physical meaning of the van't Hoff enthalpy and entropic values for cross-linked polymers, such as the poly(NIPAAm-*co*-AAc) hydrogels described here. Although, the size of the cooperative unit involved in the van't Hoff enthalpy is often unknown, the van't Hoff formalism is sensitive to subtle changes occurring in the phase transition process that are masked in a calorimetric study where the phase transition often appears as a large poorly resolved peak. Schild and Tirrell report the calorimetric ΔH° of poly(NIPAAm) to be 6.3 kJ/mol of monomer and suggested the cooperative unit is ~430 monomeric units [29]. Previous studies on the phase transition thermodynamics of poly(NIPAAm) in D_2O [14] and D_2O salt solutions [13] adopted a cooperative unit equal to the cross-linking density of the hydrogel (300:1). A similar convention is adopted in this work to allow direct comparisons with previous thermodynamic data.

Pure poly(NIPAAm) exhibits four distinct linear domains in Fig. 3, and the thermodynamic values derived from Regions I and II are consistent with previous reports by Rice [14] and Burba et al. [13]; the enthalpy and entropy of regions III and IV is not discussed in

Table 1. Enthalpy and entropy values for several poly(NIPAAm-*co*-AAc) polymers.

	ΔH^o (kJ mol^{-1})[(a)]			ΔS^o (J mol^{-1} K^{-1})[(a)]		
Region	0.0 mol% AAc	1.0 mol% AAc	2.5 mol% AAc	0.0 mol% AAc	1.0 mol% AAc	2.5 mol% AAc
I	2.00 ± 0.06	2.30 ± 0.17	1.00 ± 0.19	6.50 ± 0.19	7.46 ± 0.56	3.15 ± 0.61
II	12.09 ± 0.62	4.85 ± 0.22	3.44 ± 0.15	39.50 ± 2.02	15.78 ± 0.71	11.09 ± 0.47
III	3.40 ± 0.07	–[(b)]	–[(b)]	11.15 ± 0.22	–[(b)]	–[(b)]
IV	0.10 ± 0.01	0.41 ± 0.02	0.64 ± 0.01	0.45 ± 0.04	$1.43 \pm 0.0.07$	2.07 ± 0.04

[(a)]The thermodynamic values calculated from the van't Hoff plots (Fig. 3) were divided by the cross-linking density of the polymer (300:1) to obtain the thermodynamic parameters in terms of monomeric units.

[(b)]Region III displays marked non-linearity. Thus, thermodynamic values are not calculated for these samples.

those earlier reports. Both ΔH° and ΔS° increase slightly for region I when poly(NIPAAm) is doped with 1.0 mol% acrylic acid. In contrast, ΔH° and ΔS° for the 2.5 mol% sample is approximately half that of poly(NIPAAm) for over the same region. Although regions II, III and IV begin to merge into a continuous, non-linear curve for the 1.0 and 2.5 mol% samples, it is possible to extract statistically significant linear fits for portions of the data that correspond to regions II and IV of poly(NIPAAm). Region III is excluded from the analysis given the substantial amount of curvature evident in the van't Hoff plots. The ΔH° and ΔS° values for the 1.0 and 2.5 mol% samples are considerably lower than the corresponding value for the pure polymer. However, the thermodynamic parameters for the copolymers over region IV are slightly higher than that of poly(NIPAAm).

Recovery of the NMR Signal upon Cooling

Monitoring the recovery of the NMR signal during cooling can provide insight into the role of acrylic acid in polymer rehydration rates. Figure 4 compares heating and cooling cycles for the poly(NIPAAm-*co*-AAc) hydrogels. Pure poly(NIPAAm) exhibits temperature hysteresis between heating and cooling cycles. Indeed, the NMR signal does not begin to increase in intensity until the sample is cooled to 32°C (near the onset temperature of phase separation during the heating cycle), and the shape of the cooling curve does not match the heating curve. That is, the magnitude of the NMR signal gradually increases when the sample is cooled to 25°C. This is in stark contrast to the rapid dehydration that occurs when the polymer is heated. Much longer dwell times at each temperature point (ca. 2 h) are needed for poly(NIPAAm) to achieve equilibrium during the cooling cycle.

Acrylic acid decreases the hysteresis between heating and cooling curves and reduces dwell times required for equilibration upon cooling. For example, a 5-min dwell time

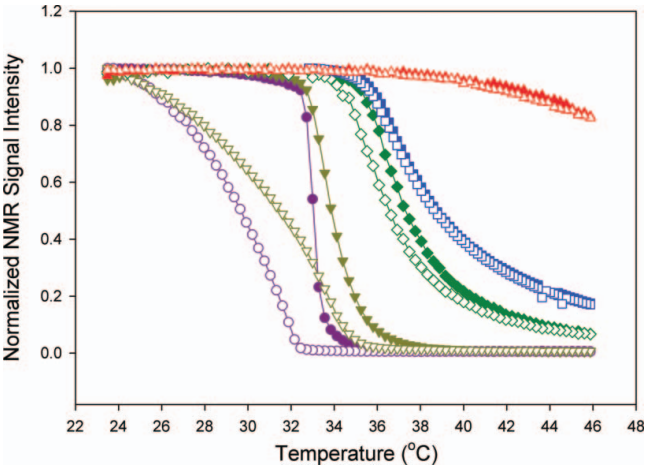

Figure 4. Temperature-dependent HRMAS ^{1}H NMR data are used to compare dehydration and rehydration rates for poly(NIPAAm-*co*-AAc) hydrogels as a function of acrylic acid content. Normalized signal intensities are reported for the methyl protons on the *N*-isopropylacrylamide substituents (δ = 1.05 ppm). Samples are denoted by the acrylic acid contents (reported in mole percent) as follows: ● = 0.0 (heating), ○ = 0.0 (cooling); ▼ = 1.0 (heating), ▽ = 1.0 (cooling); ◆ = 2.5 (heating), ◇ = 2.5 (cooling); ■ = 5.0 (heating), □ = 5.0 (cooling); and ▲ = 10.0 (heating), △ = 10.0 (cooling).

at each temperature step, which is depicted in Fig. 4, is sufficient for the 5.0 and 10.0 mol% samples to achieve equilibrium on both heating and cooling cycles. The 1.0 and 2.5 mol% samples exhibit intermediate levels of hysteresis to pure poly(NIPAAm) and poly(NIPAAm-*co*-AAc) containing 10.0 mol% acrylic acid.

Discussion

Phase Transition Thermodynamics for Poly(NIPAAm) Dehydration

HRMAS ^{1}H NMR measurements of the methyl protons from NIPAAm provide a unique perspective on how acrylic acid influences the phase transition of poly(NIPAAm). There is general consensus that dehydration of poly(NIPAAm) occurs through a series of stages and is largely controlled by (1) hydrophobic interactions of the isopropyl groups and the methylene units along the polymer backbone and (2) intra- and intermolecular hydrogen bonds among the NIPAAm monomeric units (either within a single polymer chain or between two different polymer chains, respectively) as well as intermolecular hydrogen bonds between NIPAAm and water. Ramon and co-workers [30] proposed a four-stage model for the dehydration of poly(NIPAAm) using attenuated total reflection (ATR) FT-IR spectroscopy to probe the hydrogen bonding environment of NIPAAm. The observation of a four-stage dehydration mechanism is in qualitative agreement with the van't Hoff plots in Fig. 3; however, the LCST reported by Ramon and co-workers [30] is approximately 3°C higher than what is observed in the NMR data presented in Fig. 2 and elsewhere [29].

The pre-phase transition region denoted on Fig. 3 (region I, $T < 32.5$°C) has a van't Hoff enthalpy and entropy of 2.00 kJ mol^{-1} and 6.50 J mol^{-1} K^{-1}, respectively. FT-IR spectroscopic studies suggest that poly(NIPAAm) forms extensive hydrogen bonds with water molecules at temperatures well below the phase transition temperature [30–32]. As the temperature is increased, the fraction of water-amide hydrogen bonds decreases, while the population of free, non-hydrogen-bonded amide groups increases [30]. The van't Hoff enthalpy may be attributed to the subtle changes taking place in the hydration sphere of the polymer chains over this temperature range. In addition, the van't Hoff entropy changes for region I are small but positive. Water is a good solvent for poly(NIPAAm) below the LCST. At the LCST, however, water becomes a θ-solvent. Dilute linear polymer chains adopt ideal configurations in a θ-solvent as described by their random-walk coil dimensions. For single chains of poly(NIPAAm), this is marked by a decrease in the radius of gyration [33] and an increase in the rigidity of the polymer [34]. The increase in entropy during the pre-phase transition stage is possibly due to an increase in the configurational entropy of the polymer chains as the temperature approaches the θ-temperature.

Substantial dehydration of poly(NIPAAm) occurs for temperatures corresponding to region II in Fig. 3 (32.5°C $< T < 33.3$°C). The van't Hoff enthalpy for Region II is ~12 kJ/mol, which is comparable to hydrogen bond dissociation energies. Schild and Tirrell [29] concluded that approximately one hydrogen bond per monomeric unit is lost upon dehydration of the polymer chains, and the van't Hoff ΔH° reported for this region is consistent with this assignment. The NIPAAm groups may undergo intermolecular and intramolecular hydrogen bonding through the C=O or N−H groups. Maeda et al. [32] observed a single absorption species for the amide I band in the infrared spectrum of poly(NIPAAm) below the LCST, which they assigned to C=O···H−OH interactions. The amide I band consists of ~80% C=O stretching motion and a minor amount of C-N stretching motion; therefore, it is a good spectroscopic probe of the potential energy environment about the C=O portion of the amide groups. Above the LCST, an additional band appeared in the IR spectrum that is

consistent with the presence of C=O···H−N inter- or intramolecular hydrogen bonds [32]. However, infrared spectroscopic data for the amide I band argue that the majority of the C=O groups remain hydrogen bonded to water even above the LCST. The amide II band is due to ∼60% N−H bending motion and ∼40% C−N stretching vibrations. Thus, this band is sensitive to the local environment about the N−H groups. Below the LCST, the frequency of the amide II band is consistent with N−H···OH_2 hydrogen bonds; though, an additional band appears at lower frequencies above the LCST that is assigned to intermolecular or intramolecular hydrogen bonds with the C=O groups [32]. Ramon et al. [30] observe a slight decrease in the number of free amide groups and a substantial decrease in the fraction of amide groups participating in intermolecular hydrogen bonds across this temperature range. The fraction of intramolecular hydrogen bonded amide groups increased slightly. Based on these spectroscopic observations, the enthalpy changes associated with region II are assigned to dehydration of one water molecule per N−H group of the polymer. The van't Hoff ΔS° is ∼40 J mol^{-1} K^{-1}; this increase in entropy is assigned to the release of water molecules from the polymer chains.

Infrared spectroscopic studies reveal a decrease in the intra- and intermolecular hydrogen bonded amide groups for $33.3^\circ C < T < 35.5^\circ C$ (region III), while the population of free amide groups increases to a maximum level at 35°C [30]. The van't Hoff enthalpy for this region is 3.4 kJ mol^{-1} and the van't Hoff entropy is 11.15 J mol^{-1} K^{-1}. The thermodynamic data likely reflect the breaking of additional water-amide and amide-amide hydrogen bonds as the polymer continues dehydration and the hydrophobic isopropyl groups and the polymer backbone coalesce. At the end of region III, the poly(NIPAAm) is a rigid mass, and essentially no NMR signal is observed in the HRMAS NMR spectra. Changes in the NMR data for post-phase transition temperature domain (region IV, $T > 35.5^\circ C$) are very small because most of the NIPAAm groups are dehydrated and rigid. It is difficult to make definitive statements about any changes that transpire over this temperature range since very few NIPAAm groups remain flexible enough to yield a measurable NMR signal.

Phase Transition Thermodynamics for Poly(NIPAAm-co-AAc) Dehydration

Copolymerizing NIPAAm with hydrophilic or hydrophobic molecules is known to have a dramatic effect on inter- and intramolecular hydrogen bonding interactions present among the polymer chains of the hydrogel. These interactions are the primary factors that determine the chemical and physical properties of the poly(NIPAAm)-based materials. Small quantities of acrylic acid are sufficient to affect the phase transition thermodynamics of poly(NIPAAm). Although the thermodynamic values for all of the regions denoted in Fig. 3 are affected by the acrylic acid content, the most dramatic changes are noted in regions II and III. In pure poly(NIPAAm), these regions are associated with substantial dehydration of the polymer chains. Doping poly(NIPAAm) with 1.0-mol% acrylic acid results in a 40% reduction for the region II van't Hoff ΔH° and ΔS° compared to pure poly(NIPAAm). Moreover, regions II, III and IV are less distinct in the 1.0-mol% sample and significant non-linearity in the van't Hoff plot is evident for "region III". Increasing the doping level to 2.5 mol% further reduced the van't Hoff thermodynamic values.

The reduced values of the van't Hoff ΔH° and ΔS° are attributed to the enhanced hydrophilicity of the polymer chains. Acrylic acid is more hydrophilic than NIPAAm and has a pK_a of 4.25. Thus, incorporating hydrophilic acrylic acid sites along the poly(NIPAAm) chains will enhance water-polymer interactions, leading to an increase in the LCST of the materials and a suppression of hydrogel dehydration. Feil et al. [35] established a linear relationship between calorimetric ΔH and LCST, implying that hydrophilicity of acrylic acid

does not directly impact the enthalpy of the phase transition. Instead, Feil and co-workers [35] proposed that acrylic acid increases the overall hydrophilicity of the polymer chains by reducing the total number of hydrophobic groups. The strengthened water-polymer interactions compensates any increases in the hydrophobic interactions as temperature is increased, thereby raising the LCST of the co-polymer. The authors further argue that increased LCSTs for co-polymerized samples exhibit reduced calorimetric enthalpies of the phase transition because the higher temperatures destabilize the hydration sphere around the polymer chains compared to samples with lower LCSTs.

The thermodynamic data reported in Table 1 are consistent with the model proposed by Feil et al. [35]. At low doping levels, poly(NIPAA-*co*-AAc) polymer chains consist of relatively long segments of poly(NIPAAm) interspersed with hydrophilic acrylic acid sites. These sites stabilize the hydration sphere about the polymer chains and shift the phase transition temperature to higher temperatures. At very low doping levels (<1 mol% acrylic acid), the average length of the NIPAAm segments is long, and the phase transition process is similar to that of pure poly(NIPAAm). Increased amounts of acrylic acid shortens the length of poly(NIPAAm) segments, increasing the overall effect of the acrylic acid on the water-polymer interactions. The stabilized hydration sphere around the polymer chains results in reduced numbers of water molecules being released from the hydrogel during the phase transition. The van't enthalpy and entropy values are largely controlled by the release of water molecules as the polymer is heated across the phase transition temperature. Thus, changes in the stability of water-polymer interactions appear as reductions in the van't Hoff ΔH° and ΔS°, especially for regions II and III. The van't Hoff ΔH° and ΔS° for region IV slightly increases when the acylic acid content is raised from 0.0 mol% to 2.5 mol%. This is attributed to the release of water molecules that are tightly bound to the polymer chains, possibly in the local vicinity of an acrylic acid site. The enhanced stability of the hydration sphere for acrylic acid-containing polymers leads to a larger fraction of residual water molecules bound to the polymer chains above the LCST, and higher temperatures are needed to fully dehydrate the material. The fraction of residual water becomes quite large in the case of 5.0- and 10.0-mol% samples.

Rate of NMR Signal Recovery during Rehydration of Poly(NIPAAm-co-AAc) Hydrogels

Hydration and dehydration rates of poly(NIPAAm), and its derivatives, has been extensively studied in the literature since those processes are very important for drug delivery applications, where understanding the kinetic release/uptake of pharmaceuticals is critical to hydrogel function. Early theoretical work on swelling kinetics by Tanaka and Fillmore [36] focused on the swelling behavior of spherical gels using cooperative diffusion theory. For spherically-shaped gels, the shear modulus of the network is negligible, and the relaxation time for the polymer swelling is proportional to the radius of the particle squared (i.e., $\tau \sim a^2$). Peters and Candau [37] extended the Tanaka-Fillmore model to include spherical, cylindrical and disk-like particle shapes for which the shear modulus is non-zero. Later, Li and Tanaka [38] developed a generalized form of the theory that is applicable to gels of any shape. In the more general forms, swelling kinetics is viewed as a diffusion process mediated by shape changes that serve to minimize the shear energy of the expanding polymer. Thus, swelling kinetics is not fully described by diffusion of water molecules into the polymer but must include shear effects that minimize non-isotropic deformations. The Li-Tanaka drying and swelling kinetic model has been confirmed with *in situ* interferometry measurements of thin poly(NIPAAm) films in water [39]. Furthermore, Hirose and

Shibayama found excellent agreement between the Tanaka-Fillmore model and experimental swelling kinetics for poly(NIPAAm-*co*-AAc) hydrogels. The cooperative diffusion coefficient derived from temperature-jump measurements was found to be $2.1 \times 10^{-7}\,\mathrm{cm}^2 \cdot \mathrm{s}^{-1}$ for hydrogels containing 4.8-mol% acrylic acid [40].

Quijada-Garrido et al. [41] investigated the rehydration kinetics of poly(NIPAAm-*co*-methacrylic acid) copolymers with magnetic resonance imaging. Swelling of the copolymer is hypothesized to occur through two distinct processes. The first process is the swelling of an external zone along the outer surface of the polymer, which then migrates towards the center of the polymer. Quijada-Garrido and co-workers [41] determined that movement of the hydration front towards the center of polymer follows first-order kinetics. The authors further propose an auto-acceleration mechanism is needed to fully explain the rehydration kinetics of the copolymers. In this mechanism, water molecules that have diffused into the polymer aid the diffusional of additional water molecules. This mechanism is summarized below as:

$$\mathrm{H_2O} \xrightarrow{k_1} \mathrm{H_2O^*} \tag{3}$$

$$\mathrm{H_2O} + \mathrm{H_2O^*} \xrightarrow{k_2} 2\mathrm{H_2O^*} \tag{4}$$

where H_2O^* denotes a water molecule inside the polymer. Combining both processes leads to the following integrated rate law for swelling poly(NIPAAm-*co*-methacrylic acid) [41]:

$$rate_{swelling} = \beta \left(\frac{(k_1/k_2)(1 - e^{-(k_1+k_2)t})}{k_1/k_2 + e^{-(k_1+k_2)t}} \right) + (1 - \beta)(1 - e^{-k_3 t}). \tag{5}$$

The rate constant k_3 describes the rate the hydration front moves towards the center of the polymer and β is the relative fraction both processes contribute to the swelling process. The rate constants k_1, k_2, and k_3 as well as β all depend on the composition of the copolymer.

Although a quantitative kinetic study of the rehydration process for our poly(NIPAAm-*co*-AAc) samples is not possible with the data presented in Fig. 4, qualitative changes in the rehydration rates can be explained in the context of the kinetic models given above. In the absence of acrylic acid, the onset of rehydration is approximately equal to the onset of dehydration during the heating cycle, as measured by the recovery of the NMR signal in Fig. 2. This implies that the temperature of the hydrogel must drop below the point at which the hydrophobic bonds are stable in pure poly(NIPAAm) for rehydration to occur [13, 14]. However, rehydration kinetics is much slower than the five minute dwell time used to establish thermal equilibrium in the sample. Thus, the poly(NIPAAm) sample is not full equilibrated at each temperature measurement. The addition of acrylic acid appears to somewhat remove this requirement, allowing rehydration to occur at higher temperatures. Furthermore, rehydration is faster as the acrylic acid content is increased, and the 5.0- and 10.0-mol% samples reach thermodynamic equilibrium within the 5-min dwell time.

In poly(NIPAAm), rehydration is a kinetic process that is frustrated by the hydrophobic nature of the polymer and the need to replace amide-amide bonds with amide-water bonds. Here, the rate-limiting step for rehydration is usually taken as the slow diffusion of water molecules through the collapsed gel. In poly(NIPAAm-*co*-AAc), acrylic acid tightly binds water molecules to the polymer chain, stabilizing the hydration shell at elevated temperatures and preventing the crosslinked hydrogel from fully dehydrating. Indeed, Fig. 2 shows substantial amounts of flexible NIPAAm monomeric units in copolymers containing more than 2.5 mol% acrylic acid. Thus, large quantities of residual water are retained within these

polymers above their LCSTs. This observation is further corroborated by the reduction in the van't Hoff enthalpy and entropy for poly(NIPAAm-*co*-AAc), which is interpreted as a reduced number of water-amide hydrogen bonds being broken during the phase transition. The presence of hydrated domains enables facile diffusion pathways for the water molecules, promoting faster rehydration of the crosslinked samples during the cooling cycle. In the context of the kinetic mechanism proposed by Quijada-Garrido et al. [41], the residual water molecules within the polymer appears as an increased population of H_2O^* molecules in equation 4. Thus, the auto-acceleration process becomes more important in the rehydration of these materials, increasing rehydration kinetics.

Conclusions

High-resolution magic-angle-spinning (HRMAS) ^{1}H NMR spectroscopy is used to investigate the phase transition of a series of poly(*N*-isopropylacrylamide-*co*-acrylic acid) hydrogels crosslinked with *N*,*N*′-methylene bisacrylamide, or poly(NIPAAm-*co*-AAc). The relative amounts of flexible, hydrated NIPAAm segments within the sample are directly measured by following changes in the normalized ^{1}H NMR intensity of methyl protons from the NIPAAm substituents. Thus, quantitative information concerning the relative fraction of hydrated NIPAAm domains is obtained as a function of temperature. These measurements provide insight into how acrylic acid influences the phase transition thermodynamics and kinetics from the perspective of the NIPAAm constituents. Acrylic acid causes a pronounced increase in the LCSTs of the hydrogel, which is related to differences in the hydrophilicity of acrylic acid and NIPAAm. The resulting van't Hoff enthalpy and entropy values derived from temperature-dependent NMR data of pure poly(NIPAAm) are consistent with a four-stage phase transition process.

The van't Hoff plots of poly(NIPAAm-*co*-AAc) show several qualitative differences from pure poly(NIPAAm); however, the data clearly support a multi-step phase transition process analogous to poly(NIPAAm). In addition, the phase transition thermodynamics are substantially smaller for poly(NIPAAm-*co*-AAc) than poly(NIPAAm). These differences are attributed to the presence of hydrophilic acrylic acid sites along the poly(NIPAAm) polymer chains, which enhance the stability of the hydration sphere surrounding the polymer chains. Stronger interactions between the polymer chains and water molecules increases the LCST of the hydrogel and the fraction of residual water bound to the polymer chains above the LCST. These two effects reduce the number of water-amide hydrogen bonds broken during the phase transition process and lead to smaller van't Hoff thermodynamic values.

The presence of acrylic acid in poly(NIPAAm) has a significant influence on the rehydration kinetics of the collapsed polymer. The rate-limiting step for rehydration is believed to be the slow diffusion of water molecules through the collapsed gel. Acrylic acid prevents the crosslinked hydrogel from fully dehydrating at elevated temperatures, leaving a significant fraction of water molecules within the hydrogel. These residual water molecules promote facile diffusion of water into the bulk of the sample and, thus, accelerate the rehydration kinetics of these materials.

Acknowledgments

This work was supported by the University of Oklahoma and a CAREER Award from the National Science Foundation to CVR (CHE-0449622). CMB is indebted to Northeastern State University for partial support of the project.

References

[1] Peppas, N. A., Huang, Y., Torres-Lugo, M., Ward, J. H., & Zhang, J. (2000). *Ann. Rev. Biomed. Eng.*, *2*, 9.
[2] Mori, T., & Maeda, M. (2004). *Langmuir*, *20*, 313.
[3] Lee, K. Y., & Mooney, D. J. (2001). *Chem. Rev.*, *101*, 1869.
[4] Schmidt, C. E., & Leach, J. B. (2003). *Ann. Rev. Biomed. Eng.*, *5*.
[5] Vogel, V., & Baneyx, G. (2003). *Ann. Rev. Biomed. Eng.*, *5*.
[6] Griffith, L. G., & Naughton, G. (2002). *Science*, *295*, 1009.
[7] Hench, L. L., & Polak J. M. (2002). *Science*, *295*, 1014.
[8] Schild, H.G. (1992). *Prog. Polym. Sci.*, *17*, 163.
[9] Stile, R. A., Burghardt, W. R., & Healy, K.E. (1999). *Macromolecules*, *32*, 7370.
[10] Stile, R. A., & Healy, K. E. (2001). *Biomacromolecules*, *2*, 185.
[11] Yin, X., Hoffman, A. S., & Stayton, P. S. (2006). *Biomacromolecules*, *7*, 1381.
[12] Feil, H., Bae, Y. H., Feijen, J., & Kim, S.W. (1992). *Macromolecules*, *25*, 5528.
[13] Burba, C. M., Carter, S. M., Meyer, K. J., & Rice, C.V. (2008). *J. Phys. Chem. B*, *112*, 10399.
[14] Rice, C.V. (2006). *Biomacromolecules*, *7*, 2923.
[15] Keifer, P. A., Baltusis, L., Rice, D. M., Tymiak, A. A., & Shoolery, J. N. (1996). *J. Magn. Reson. Ser. A*, *119*, 65.
[16] Fitch, W. L., Detre, G., Holmes, C. P., Shoolery, J. N., & Keifer, P.A. (1994). *J. Org. Chem.*, *59*, 7955.
[17] Elbayed, K., Dillmann, B., Raya, J., Piotto, M., & Engelke F. (2005). *J. Magn. Reson.*, *174*, 2.
[18] Piotto, M., Elbayed, K., Wieruszeski, J.-M., & Lippens, G. (2005). *J. Magn. Reson.*, *173*, 84.
[19] Hoffman, R. E., & Becker E. D. (2005). *J. Magn. Reson.*, *176*, 87.
[20] Doty, F. D., Entzminger, G., & Yang, Y. A. (1998). *Concepts Magn. Reson.*, *10*, 239.
[21] Chen, G., & Hoffman, A. S. (1995). *Nature*, *373*, 49.
[22] Bokias, G., Staikos, G., & Iliopoulos, I. (2000). *Polymer*, *41*, 7399.
[23] Taylor, L. D., Cerankowski, L. D. (1975). *J. Poly. Sci.*, *13*, 2551.
[24] Maeda, Y., Higuchi, T., & Ikeda, I. (2001). *Langmuir*, *17*, 7535.
[25] Maeda, Y., Tsubota, M., & Ikeda, I. (2003). *Colloid Poly. Sci.*, *281*, 79.
[26] Tiera, M. J., dos Santos, G. R., de Oliveira Tiera, V. A., Vieira, N. A. B., Frolini, E., da Silva, R. C., & Loh, W. (2005). *Colloid Poly. Sci.*, *283*, 662.
[27] Principi, T., Goh, C. C. E., Liu, R. C. W., & Winnik, F. M. (2000). *Macromolecules*, *33*, 2958.
[28] Sutherland, J. W. H. (1977). *Proc. Natl. Acad. Sci.*, *74*, 2002.
[29] Schild, H. G., & Tirrell, D. A. (1990). *J. Phys. Chem.*, *94*, 4352.
[30] Ramon, O., Kesselman, E., Berkovici, R., Cohen, Y., & Paz, Y. (2001). *J. Poly. Sci. Part B*, *39*, 1665.
[31] Lin, S.-Y., Chen, K.-S., & Run-Chu, L. (1999). *Polymer*, *40*, 2619.
[32] Maeda, Y., Higuchi, T., & Ikeda, I. (2000). *Langmuir*, *16*, 7503.
[33] Wu, C., & Zhou, S. (1998). *Macromolecules*, *28*, 8381.
[34] Hsu, S.-H., & Yu, T.-L. (2000). *Macromol. Rapid Commun.*, *21*, 476.
[35] Feil, H., Bae, Y. H., Feijen, J., & Kim, S. W. (1993). *Macromolecules*, *26*, 2496.
[36] Tanaka, T., & Fillmore, D. J. (1979). *J. Chem. Phys.*, *70*, 1214.
[37] Peters, A., & Candau, S. J. (1988). *Macromolecules*, *2*, 2278.
[38] Li, Y., & Tanaka, T. (1990). *J. Chem. Phys.*, *92*, 1365.
[39] Zhou, S., & Wu, C. (1996). *Macromolecules*, *29*, 4998.
[40] Hirose, H., & Shibayama, M. (1998). *Macromolecules*, *31*, 5336.
[41] Quijada-Garrido, I., Prior-Cabanillas, A., Garrido, L., & Barrales-Rienda, J. M. (2005). *Macromolecules*, *38*, 7434.